J Physiol Sci (2013) 63:345–353
DOI 10.1007/s12576-013-0270-y

ORIGINAL PAPER

Lobe-related concentration- and Ca^{2+}-dependent interactions of calmodulin with C- and N-terminal tails of the $Ca_V1.2$ channel

Guilin He · Feng Guo · Tong Zhu · Dongxue Shao · Rui Feng · Dandan Yin · Xuefei Sun · Huiyuan Hu · Ahhyeon Hwang · Etsuko Minobe · Masaki Kameyama · Liying Hao

Received: 19 March 2013 / Accepted: 16 May 2013 / Published online: 4 June 2013

Abstract This study examined the bindings of calmodulin (CaM) and its mutants with the C- and N-terminal tails of the voltage-gated Ca^{2+} channel $Ca_V1.2$ at different CaM and Ca^{2+} concentrations ($[Ca^{2+}]$) by using the pull-down assay method to obtain basic information on the binding mode, including its concentration- and Ca^{2+}-dependencies. Our data show that more than one CaM molecule could bind to the $Ca_V1.2$ C-terminal tail at high $[Ca^{2+}]$. Additionally, the C-lobe of CaM is highly critical in sensing the change of $[Ca^{2+}]$ in its binding to the C-terminal tail of $Ca_V1.2$, and the binding between CaM and the N-terminal tail of $Ca_V1.2$ requires high $[Ca^{2+}]$. Our data provide new details on the interactions between CaM and the $Ca_V1.2$ channel.

Keywords Calmodulin · Ca^{2+} · $Ca_V1.2$ · Binding · Affinity

G. He · F. Guo · D. Shao · R. Feng · D. Yin · X. Sun · H. Hu · A. Hwang · L. Hao (✉)
Department of Pharmaceutical Toxicology, School of Pharmaceutical Science, China Medical University, Shenyang 110001, China
e-mail: lyhao@mail.cmu.edu.cn

G. He · F. Guo · D. Shao · R. Feng · D. Yin · X. Sun · H. Hu · A. Hwang · L. Hao
Cardiovascular Institute of China Medical University, Shenyang 110001, China

T. Zhu
Laboratory of Environmental Biology, Northeastern University, Shenyang 110004, China

E. Minobe · M. Kameyama
Department of Physiology, Graduate School of Medical and Dental Sciences, Kagoshima University, Kagoshima 890-8544, Japan

Introduction

Voltage-gated Ca^{2+} channels (Ca_Vs) control cellular Ca^{2+} entry in response to changes in the membrane potential, and play essential roles in the generation of cardiac action potentials, excitation–contraction coupling, hormone and neurotransmitter release, and activity-dependent gene transcription [1]. Ca^{2+} is not only a potent activator of intracellular signaling pathways but also a toxicant when overloaded [2]. As the major routes of Ca^{2+} influx, the Ca_Vs are regulated by two self-regulatory Ca^{2+}-dependent feedback mechanisms, Ca^{2+}-dependent facilitation (CDF) and Ca^{2+}-dependent inactivation (CDI) [1, 3]. CDF is an increase in the channel opening when basal Ca^{2+} level is moderately increased or repeated transient depolarization occurs, which may augment the Ca^{2+} signal, whereas CDI is an enhancement of the channel closing when the entry of Ca^{2+} is further increased, which may prevent the harmful actions of Ca^{2+} overload [1]. Calmodulin (CaM) is a ubiquitously expressed Ca^{2+}-binding protein [2], and it is believed that both CDF and CDI require CaM to bind with the α_1 subunit of Ca_Vs [3]. Especially, it has recently been demonstrated that the binding between CaM and the $Ca_V1.2$ channel and the induced Ca^{2+}-dependent regulations play very important roles not only in physiological functions but also in pathophysiological conditions [4].

Numerous studies have suggested that CaM is constitutively tethered to the channel, and that the interaction of CaM with the proximal part of the C-terminal tail of the channel plays a prominent role in CDF and CDI [5–8]. The tethering or binding sites in the C-terminal tail of $Ca_V1.2$ include an isoleucine–glutamine motif [5–7] (referred as the IQ motif, a consensus CaM-binding motif in many proteins) and a preIQ motif (also referred as peptide A and C) [5, 8] (Fig. 1a). The location of the preIQ motif is

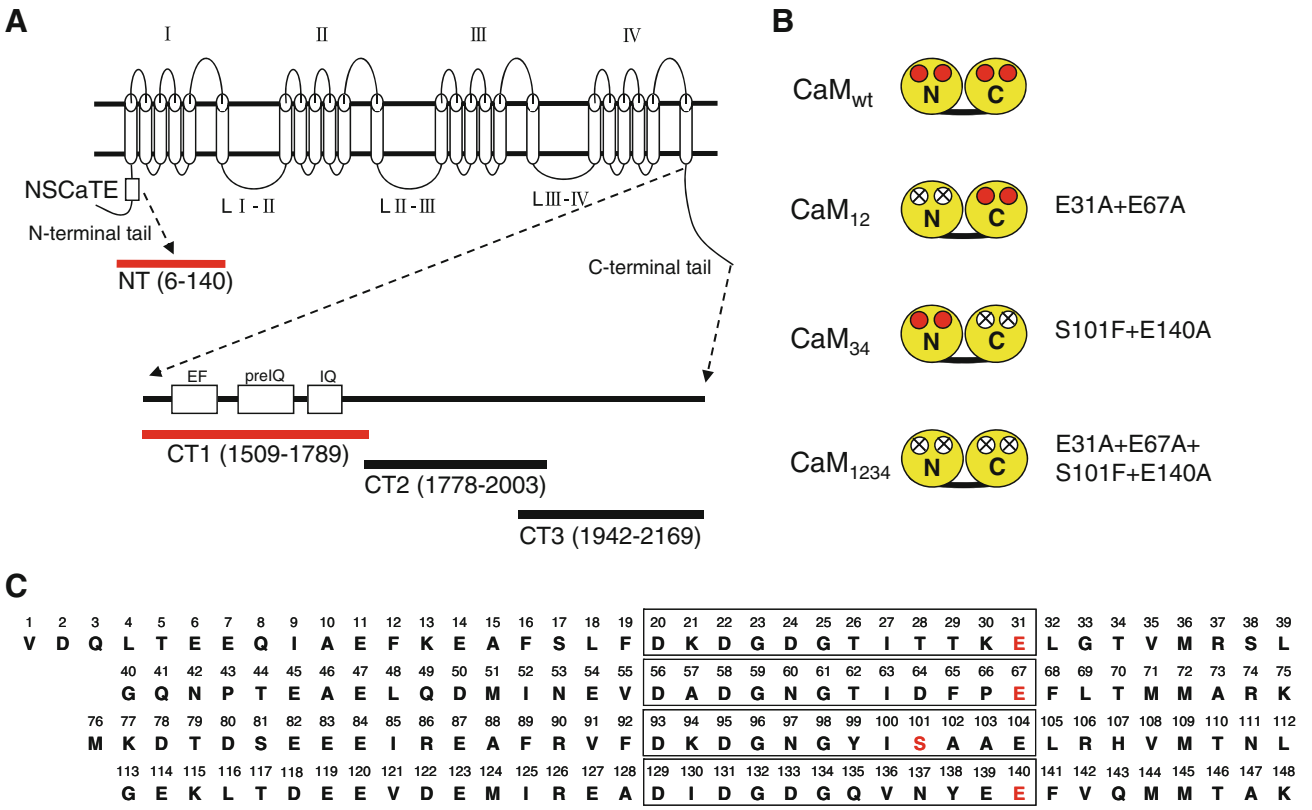

Fig. 1 Schematic illustrations of the peptides of $Ca_V1.2$ channel, CaM and its mutants. **a** NT is a N-terminal peptide containing a CaM-binding site called NSCaTE (see text). The C-terminal tail was divided into three parts as illustrated. CT1 contains regulatory regions (shown as *boxes*), Ca^{2+}-binding EF-hand motif (EF) and two CaM-binding motifs (preIQ and IQ). Amino acid (a.a.) numbers (guinea-pig cardiac $Ca_V1.2$) of peptides are shown in the *parentheses*. LI–II, LII–III and LIII–IV represent intracellular loops between homologous repeats of I to IV. **b** Schematic illustrations of CaM and its mutants (CaM_{12}, CaM_{34} and CaM_{1234}). *Closed circles* represent normal Ca^{2+}-binding sites in N-lobe (N) and C-lobe (C) of CaM, *open circles* with X represent mutated Ca^{2+}-binding sites, which are unable to bind with Ca^{2+}. Substitutions of a.a. are shown with one-letter codes of a.a. **c** A.a. sequences of human CaM. The sequences of Ca^{2+}-binding sites 1–4 and mutated points are shown in *boxes* and *red color*, respectively (color figure online)

between the IQ motif and the Ca^{2+}-binding helix-loop-helix structural motif called 'EF-hand motif' in the C-terminal tail of $Ca_V1.2$ (Fig. 1a). Besides the CaM binding sites in the C-terminal tail of $Ca_V1.2$, other regions have also been defined, including the I–II loop [8] and a CaM-binding motif in the N-terminal tail of $Ca_V1.2$ and $Ca_V1.3$, named N-terminal Spatial Ca^{2+} Transforming Element (NSCaTE) [9] (Fig. 1a). However, a report has shown that CaM cannot foster interactions between the N- and C-terminal tails to promote CDI [10]. CaM may show three different Ca^{2+}-binding states, namely, the Ca^{2+}-free form (apoCaM), and the partially and fully Ca^{2+}-bound forms (Ca^{2+}/CaM: Ca_2^{2+}CaM and Ca_4^{2+}CaM, respectively), which are likely to be physiologically relevant [2, 5, 6]. It is reported that apoCaM may bind to the C-terminal tail of $Ca_V1.2$ [5], showing that CaM may already tether to the channel even at resting condition, but it is not clear whether apoCaM may bind to the N-terminal tail of $Ca_V1.2$ or not. Thus, further work is needed to delineate the interaction of CaM with the N-terminal tail of $Ca_V1.2$ and its Ca^{2+}-dependent characteristics.

The concentration of the intracellular free Ca^{2+} at resting condition ($\sim 10^{-7}$ M) is 10^4 times lower than those outside the cells or in the intracellular stores ($\sim 10^{-3}$ M) [2]. Various extracellular stimuli promote the influx or release of Ca^{2+} from either outside the cells or the intracellular stores into the intracellular milieu. This increased intracellular Ca^{2+} is only briefly available to act as a cellular signal because Ca^{2+}-binding proteins and Ca^{2+} pumps immediately combine to sequester and transport it to intracellular storage sites or outside the cell. Structurally, a CaM has two lobes, each of which contains two EF-hand conformational Ca^{2+}-binding sites (Fig. 1b). The two Ca^{2+}-binding sites of the C-terminal lobe (C-lobe) have 3- to 5-fold higher affinity for Ca^{2+} than those of the N-terminal lobe (N-lobe) [2]. CaM mutants, such as CaM_{12} (mutated at Ca^{2+}-binding sites 1 and 2 in the N-lobe), CaM_{34} (mutated at sites 3 and 4 in the C-lobe), and

CaM_{1234} (mutated all sites above) (Fig. 1b, c), are thought to represent different Ca^{2+}-binding states of CaM, and have been used to investigate Ca^{2+}-dependent regulation of $Ca_V1.2$ channel [5, 6]. A number of experiments have demonstrated that CDF and CDI are controlled independently by the N- and C-lobes [6, 11, 12]. However, the mechanism underlying CaM lobe-specific regulations of the $Ca_V1.2$ channel remains to be settled.

Another critical issue in understanding the machinery of CDF and CDI is to deduce how many CaM molecules are involved in the Ca^{2+}-dependent regulations. Mori et al. [13] reported that one CaM appears to be both necessary and sufficient to produce CDI of its associated channel. However, a recent crystallographic study provided evidence for multiple CaM molecules binding to the preIQ–IQ region of $Ca_V1.2$ [14]. Thus, although it has been established that CaM binds to the $Ca_V1.2$ channel at multiple sites, it is not fully understood how CaM interacts with the channel during Ca^{2+}-dependent regulation.

In the present study, we have examined the bindings of CaM and its Ca^{2+}-binding site mutants to the C- and N-terminal tails of the $Ca_V1.2$ channel at different CaM concentrations and different $[Ca^{2+}]$ by using a semi-quantitative pull-down method. We have found that CaM bound to C-terminal tail in a Ca^{2+}-dependent manner in which the C-lobe of CaM is much critical for sensing the change of Ca^{2+} concentration, and more than one molecule of CaM could bind to the $Ca_V1.2$ C-terminal region at high $[Ca^{2+}]$. Our data provide new and basic information on the interaction between CaM and $Ca_V1.2$ channel.

Materials and methods

Preparation of GST-fusion peptides of $Ca_V1.2$ channel

The cDNAs corresponding to three C-terminal fragments of guinea pig $Ca_V1.2$ channel (CT1, a.a.1,509–1,789; CT2, a.a.1,778–2,003; CT3, a.a.1,942–2,169; GenBank AB016287) and nearly full-length N-terminal tail (NT, a.a.6–140) were cloned into the pGEX6P-3 plasmid (GE Healthcare Biosciences) (Fig. 1a). The corresponding peptides were expressed as GST-fusion proteins in *Escherichia coli* BL21 (DE3). Due to the limited solubility of the α_{1C} fragments, in particular CT1, the bacterial precipitates were rotated with 1.5 % N-lauroylsarcosine sodium salt (Sigma-Aldrich) for 30 min at 4 °C [15, 16]. The fusion proteins were purified with Glutathione Sepharose 4B beads (GS-4B; GE Healthcare Biosciences). The purified peptides were analyzed by SDS-PAGE, and quantified by Bradford assay using bovine serum albumin (BSA) as standard.

Preparation of CaM and its mutants

The plasmids of CaM were constructed with the cDNAs of human CaM cloned from HEK293 and pGEX6P-3 vector (GE Healthcare). Point mutations in the Ca^{2+}-binding sites of CaM were introduced by Quickchange™ site-directed mutagenesis kit (QIAGEN). CaM and its mutants CaM_{12}, CaM_{34}, and CaM_{1234}, mutated as E31A + E67A, S101F + E140A and E31A + E67A + S101F + E140A, respectively (Fig. 1b, c), were expressed and purified similarly to the peptides mentioned above. The GST regions were cleaved by PreScission protease (GE Healthcare). The purified peptides were checked by SDS-PAGE and quantified by Bradford assay using BSA as standard.

Binding assay and data analyses

The interactions of CaM and its mutants with the CT1, CT2, CT3, and NT regions of $Ca_V1.2$ channel were examined at different CaM concentrations (0.1, 0.35, 0.7, 1.4, 2.1, 3.5, 10, and 50 μM) and different free Ca^{2+} concentrations ($[Ca^{2+}] \approx$ free, 100 nM, 10 μM, and 2 mM), using a semi-quantitative GST pull-down assay. The $[Ca^{2+}]$ was calculated by using WEBMAXC v2.10 software. Accordingly, the test solutions containing free, 100 nM, and 10 μM Ca^{2+} were prepared with 5 mM EGTA and 0, 4.79, 5.01 mM $CaCl_2$, respectively; the test solution of 2 mM Ca^{2+} was prepared without EGTA and with 2 mM $CaCl_2$ in Tris buffer (50 mM Tris, 150 mM NaCl, pH 8.0). GST-fusion fragments of the $Ca_V1.2$ channel (2–4 μg) were immobilized onto GS-4B beads and incubated with CaM or its mutants in 300 μl of Tris buffer for 4 h at 4 °C under agitation. Then, the beads were gently washed twice with the same buffer containing the non-ionic detergent Tween 20 (0.05 %, Sigma-Aldrich), as previously described [15]. Bound CaM and α_{1C} peptides were resuspended in SDS sample loading buffer and applied to 15 % SDS-PAGE. Proteins were visualized by Coomassie brilliant blue R (CBB) staining. Peptide amounts in SDS-PAGE gel were quantified by scanning the bands with the Photoshop software (Adobe, San Jose, CA, USA), and the optical density was analyzed by software Image J (NIH, Bethesda, MD, USA). The standard curves were generated with authentic BSA. The concentrations of CaM and GST-fusion peptides were corrected based on the relative optical densities of 0.59 and 0.80 estimated with the same amount of CaM and GST on the gel in reference to BSA, respectively [16].

Curve fitting of the total bound [CaM] was performed with the software SigmaPlot 10.0, assuming that free [CaM] in our experimental conditions is nearly equal to

total [CaM]. According to the law of mass action, bound [CaM] (Y) in the one-site model is expressed by the Hill equation as follows.

$$Y = B_{\max} \cdot \frac{X}{K_d + X}$$

where $B_{\max}$ is the maximum binding, X is the concentration of the free ligand, and K_d is the apparent dissociation constant.

In the case of the two-site model, a sum of two Hill's equations was used to assume independent binding.

$$Y = B_{\max_1} \cdot \frac{X}{K_{d_1} + X} + B_{\max_2} \cdot \frac{X}{K_{d_2} + X}$$

where $B_{\max_1}$, K_{d_1}, $B_{\max_2}$, and K_{d_2} denote $B_{\max}$ and K_d for the high and low affinity sites, respectively.

Data are presented as means ± standard errors (SE). Student's t test was used to evaluate the statistical significance and $P < 0.05$ was considered significant.

Results

Concentration- and Ca^{2+}-dependent binding of wild type CaM to the C-terminal tail of $Ca_V1.2$

We prepared three GST-fusion peptides derived from the C-terminal tail of $Ca_V1.2$: CT1 (proximal), CT2 (middle), and CT3 (distal) (Fig. 1a). CT1 contained the EF-hand, preIQ, and IQ motifs, with the latter two being known to interact with CaM (Fig. 1a). We investigated the bindings of CaM to the three fragments of the $Ca_V1.2$ at different CaM concentrations and different [Ca^{2+}] by using a semi-quantitative pull-down assay method. In the control, CaM binding to GST was negligible (data not shown). CaM binding to CT1 was evident, while the binding to CT2 or CT3 was hardly detected (data not shown). These results are consistent with previous reports [5, 8, 15, 16]. Therefore, the following experiments were focused on the CT1 peptide.

The examples of CaM binding with CT1 are shown in Fig. 2a. CaM at various concentrations (0.1–50 μM) was incubated with GST-fusion CT1 peptide in the presence of Ca^{2+} ranging from free (unavailable for binding) to 2 mM. The binding of CaM to the GST-fusion CT1 peptide increased with increasing concentrations of CaM at any [Ca^{2+}] including the Ca^{2+}-free condition, and it increased with increasing [Ca^{2+}] at fixed CaM concentration.

Figure 2b shows the plots of bound CaM against total [CaM] along with the fitted curves. The parameters for the fitted curves are shown in Table 1. In Ca^{2+}-free condition and 100 nM Ca^{2+}, the binding between CaM and CT1 appeared to follow the one-site model. At 10 μM and 2 mM Ca^{2+}, the bindings of CaM to CT1 were better fitted by the two-site model. The maximal binding, estimated as $B_{\max_1} + B_{\max_2}$, is less than 1 mol/mol CaM/peptide at free and 100 nM Ca^{2+}, suggesting that one $Ca_V1.2$ channel peptide might bind one CaM molecule. When [Ca^{2+}] was increased, the maximal binding reaches over 1 mol/mol CaM/peptide (1.02 for 10 μM, 1.74 for 2 mM Ca^{2+}), suggesting that CT1 could bind more than one CaM molecule at higher [Ca^{2+}] (≥10 μM). The above results demonstrated that the binding of CaM to CT1 was dependent on the concentrations of both CaM and Ca^{2+}.

Concentration- and Ca^{2+}-dependent binding of CaM_{12} to CT1

The bindings of CaM_{12} to CT1 were then examined. As shown in Fig. 2c, CaM_{12} was able to bind CT1 in a concentration-dependent manner, and although less obvious than for the wild-type CaM, the Ca^{2+}-dependency was maintained. As shown in Fig. 2d, the fitted curves shift upward, indicating that the Ca^{2+}-dependency of CaM_{12} binding to CT1 still exists. Similarly to the binding features of wild-type CaM, at free and 100 nM Ca^{2+}, the one-site model is proper to describe the binding dynamics, while at 10 μM and 2 mM Ca^{2+}, the two-site model is more appropriate.

Concentration- and Ca^{2+}-dependent binding of CaM_{34} and CaM_{1234} to CT1

The bindings of CaM_{34} and CaM_{1234} were also examined. As shown in Fig. 3, these two mutated CaM were still able to bind to CT1 in a concentration-dependent manner but not in a Ca^{2+}-dependent manner. The bindings of the two mutated CaM to CT1 were up to 1 mol/mol (CaMs/CT1), implying that their binding capability was not much affected (Fig. 3b, d).

The bindings of CaM_{34} and CaM_{1234} could be fitted well with the two-site model, and the parameters obtained (Table 1) revealed that not only K_d values but also $B_{\max}$ values had no obvious Ca^{2+}-dependent change, suggesting that the C-lobe of CaM may be critical for the Ca^{2+}-dependent binding of CaM to CT1.

Concentration- and Ca^{2+}-dependent binding of CaM and its mutants to NT

Dick et al. [9] have reported that CaM could bridge the N- and C-terminal tails of $Ca_V1.2$ channels to control CDI, but Benmocha et al. [10] indicated that CaM did not foster an interaction between the CaM-binding peptides of N- and C-terminal tails. Thus, we examined the bindings of CaM and its mutants (CaM_{1234} and CaM_{34}) to NT, the

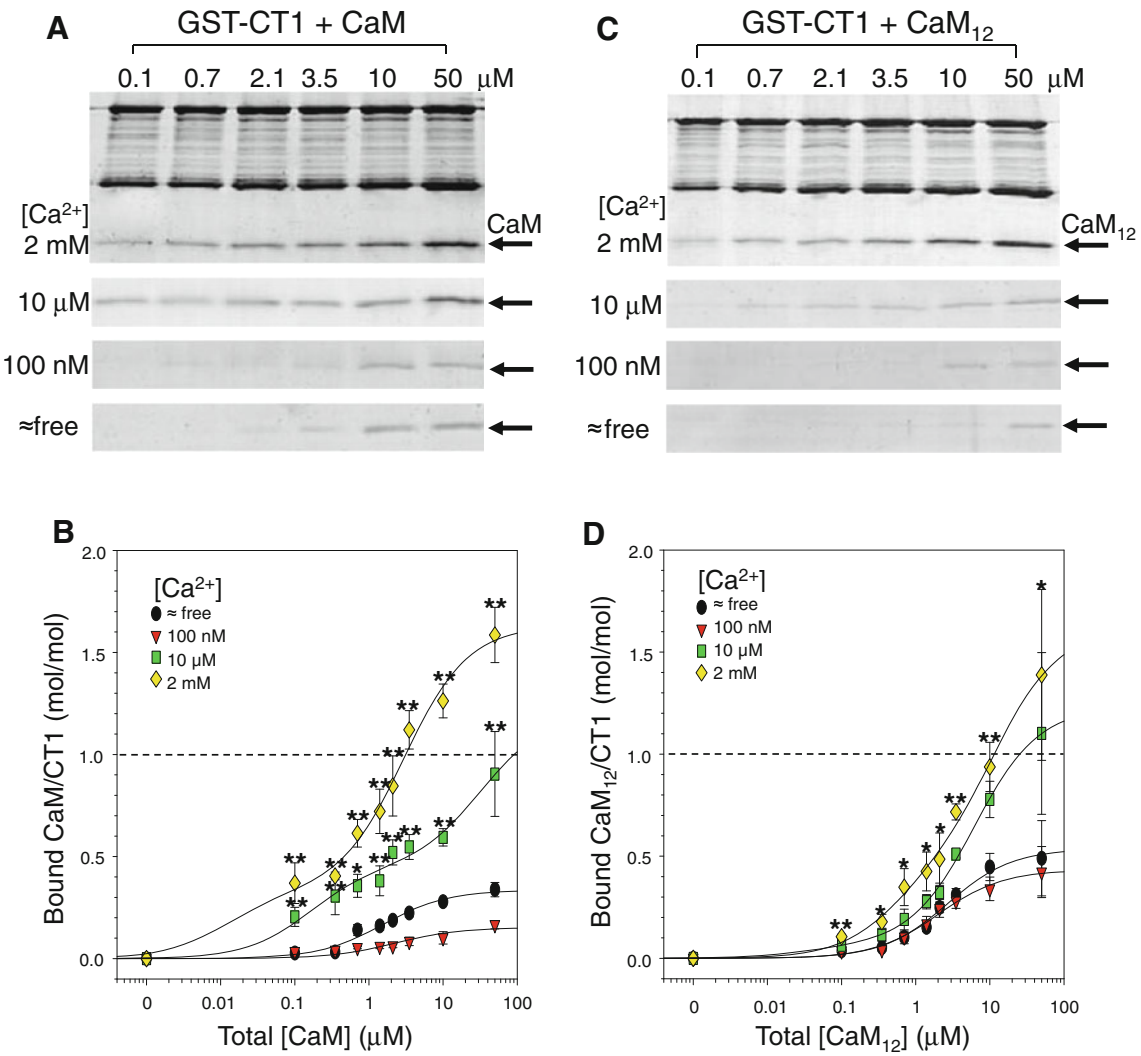

Fig. 2 CaM and CaM_{12} binding to CT1 peptide of the $Ca_V1.2$ channel. GST pull-down assay for CaM (**a**) or CaM_{12} (**c**) binding to CT1. Protein bands are shown as Coomassie brilliant blue (CBB) staining at different $[Ca^{2+}]$. CaM bands are indicated by *arrows*. Plots of concentration-dependent binding with fitted curves for CaM (**b**) and CaM_{12} (**d**) (0.1–50 μM) to CT1 at ≈free, 100 nM, 10 μM, and 2 mM Ca^{2+}. Band densities were converted into molar ratio (CaM/GST-CT1) and plotted against total [CaM] or $[CaM_{12}]$ with *symbols* as indicated in each graph and with mean ± SE ($n = 3$–10). $^*P < 0.05$, $^{**}P < 0.01$, compared with corresponding bindings at Ca^{2+}-free condition

GST-fusion peptide of $Ca_V1.2$ N-terminal tail, to investigate whether CaM is possible to bind the $Ca_V1.2$ N-terminal tail with its N-lobe. We found that CaM and the mutants did not show clear binding to NT at low $[Ca^{2+}]$ (≈free and 100 nM). When $[Ca^{2+}]$ was increased to 10 μM and 2 mM, CaM but not CaM_{1234} showed binding to NT (Fig. 4a), indicating that the binding between CaM and NT was Ca^{2+}-dependent. The curves of CaM's binding to NT were appropriately fitted with the one-site model (Fig. 4b), and the estimated B_{max} and K_d values are summarized in Table 2. CaM_{34}, in which Ca^{2+} binding is thought to be restricted to the N-lobe, also showed detectable binding to NT in the presence of Ca^{2+} (10 μM and 2 mM) (Fig. 4c, d; Table 2), implying that the N-lobe of CaM may play an important role in the binding of CaM to the N-terminal tail of $Ca_V1.2$.

Discussion

In the present study, we have investigated the concentration- and Ca^{2+}-dependencies of CaM binding with $Ca_V1.2$. It has been reported that more than one region in the C-terminal tail of $Ca_V1.2$ can bind CaM [3, 5, 8]. However, Xiong et al. [17] showed that, although synthetic short peptides could bind CaM, longer fragments could also bind to only one CaM molecule, suggesting that only one of these sequences binds CaM in the larger protein or that all

Table 1 Parameters for the bindings of CaM and its mutants to CT1

	CaM				CaM_{12}				CaM_{34}				CaM_{1234}			
	EGTA	100 nM	10 μM	2 mM	EGTA	100 nM	10 μM	2 mM	EGTA	100 nM	10 μM	2 mM	EGTA	100 nM	10 μM	2 mM
K_{d_1} (μM)	1.17	2.19	0.40	0.39	2.73	2.00	3.19	1.48	2.64	3.90	2.45	2.54	3.07	3.39	2.53	2.41
B_{max_1} (mol/mol)	0.28	0.15	0.58	0.91	0.54	0.43	0.85	0.84	0.60	0.70	0.61	0.70	0.70	0.70	0.63	0.62
K_{d_2} (μM)			33.27	10.92			29.67	25.30	6.93	7.08	7.44	6.75	6.93	9.44	8.70	7.03
B_{max_2} (mol/mol)			0.44	0.83			0.49	0.83	0.51	0.57	0.61	0.64	0.35	0.62	0.63	0.62
R^2	0.977	0.843	0.928	0.961	0.987	0.986	0.995	0.990	0.974	0.978	0.994	0.968	0.973	0.958	0.946	0.969

Data from the GST pull-down assay shown in Figs. 2, 3 were analyzed with a software SigmaPlot 10.0 and with single or double Hill equations (see "Materials and Methods"). K_{d_1} and K_{d_2}: apparent dissociation constants, B_{max_1} and B_{max_2}: the maximum bindings, R^2: coefficient of determination. Blanks in K_{d_2} and B_{max_2} meant a better fit with the single-site model than the double-site model

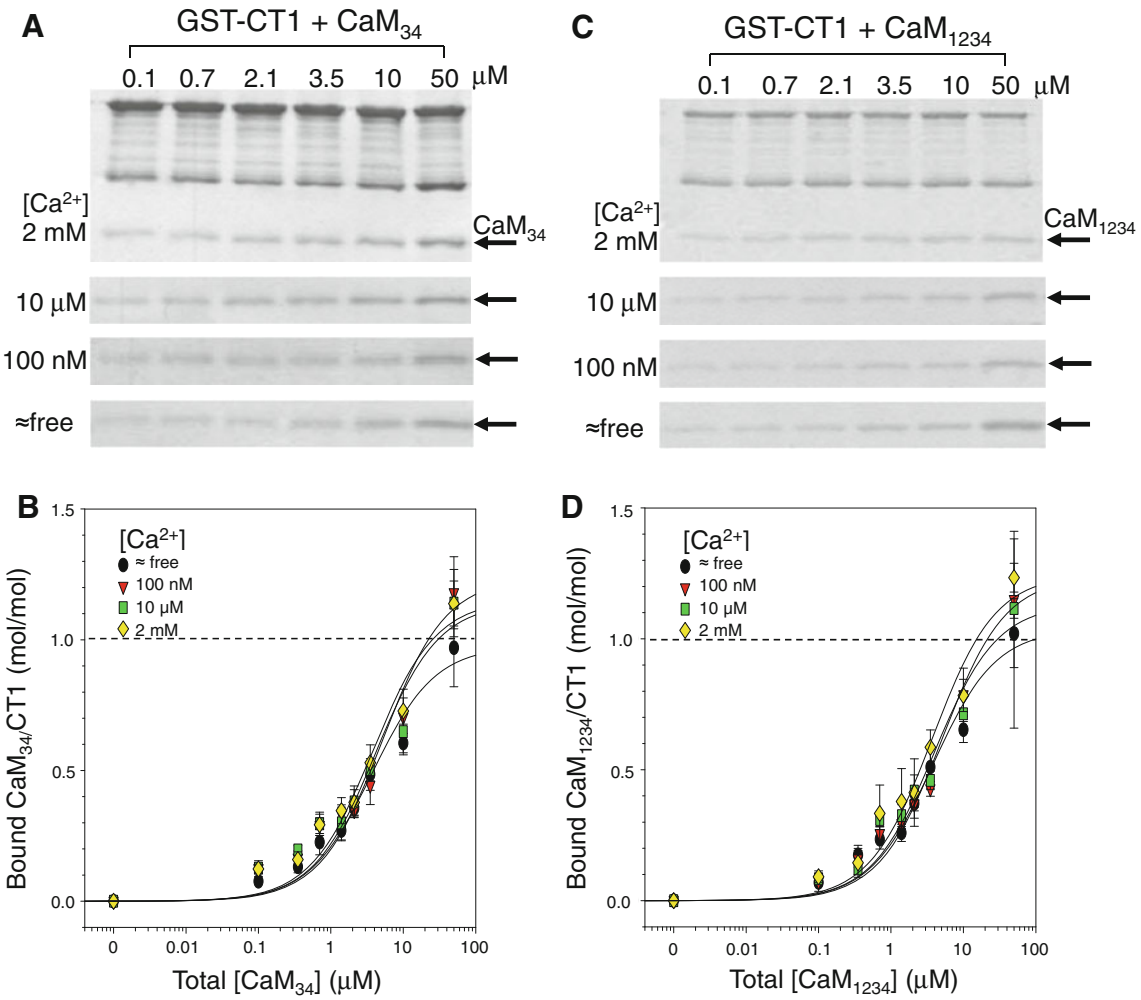

Fig. 3 CaM_{34} and CaM_{1234} binding to CT1 peptide of the $Ca_V1.2$ channel. GST pull-down assay for CaM_{34} (**a**) or CaM_{1234} (**c**) binding to CT1. Protein bands are shown as CBB staining at different $[Ca^{2+}]$. CaM bands are indicated by *arrows*. Plots of concentration-dependent binding with fitted curves of CaM_{34} (**b**) and CaM_{1234} (**d**) (0.1–50 μM) to CT1 at ≈ free, 100 nM, 10 μM and 2 mM Ca^{2+}. Band densities were converted into molar ratio (CaM_{34}/GST-CT1) and plotted against total $[CaM_{34}]$ or $[CaM_{1234}]$ with *symbols* as indicated in each graph and with mean ± SE (n = 3–10)

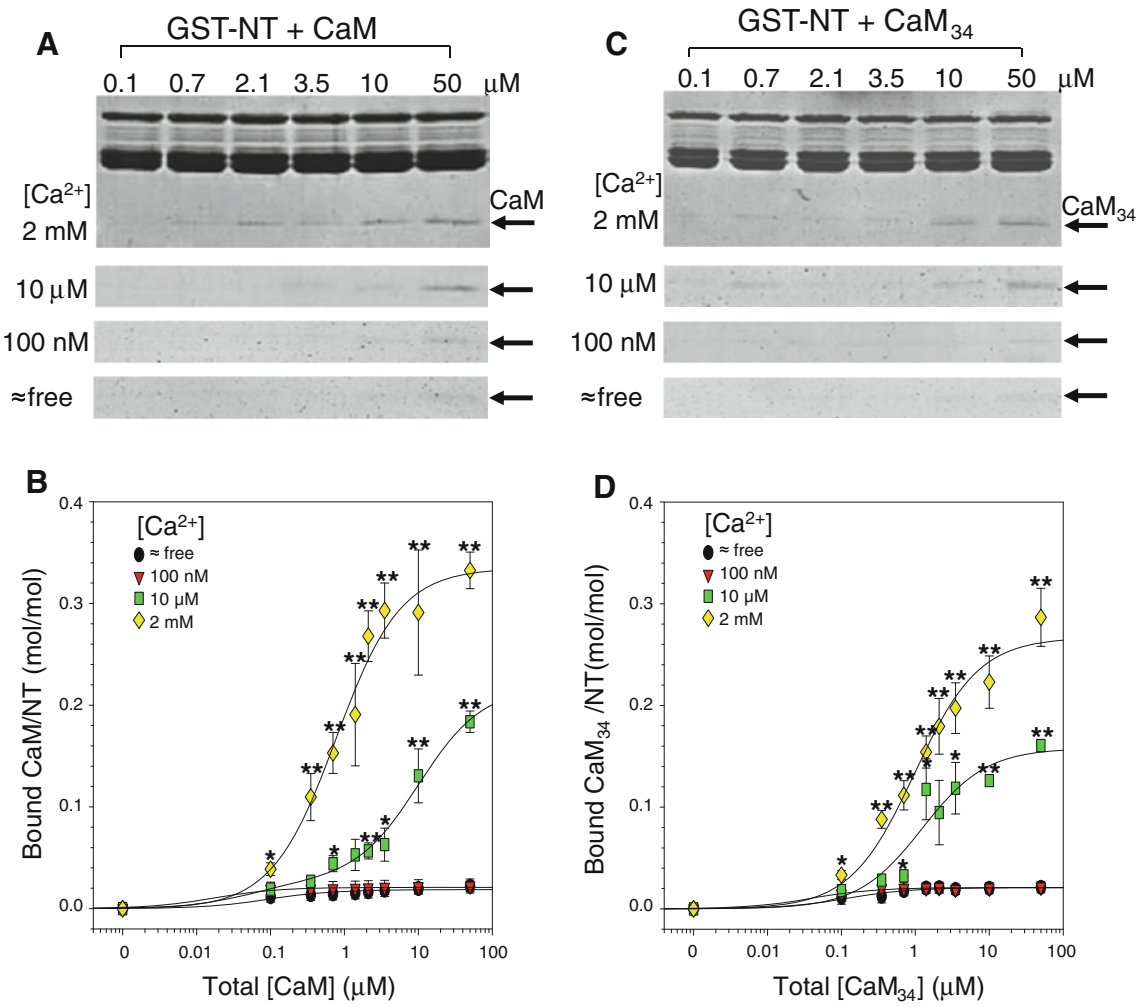

Fig. 4 CaM and CaM_{34} binding to the NT peptide of the $Ca_V1.2$ channel N-terminus. GST pull-down assay for CaM (**a**) or CaM_{34} (**c**) binding to NT. Protein bands are shown as CBB staining at different $[Ca^{2+}]$. CaM bands are indicated by *arrows*. Plots of concentration-dependent binding with fitted curves of CaM (**b**) or CaM_{34} (**d**) (0.1–50 μM) to NT at free, 100 nM, 10 μM and 2 mM Ca^{2+}. Band densities were converted into molar ratio (CaM/GST-NT) and plotted against total [CaM] or $[CaM_{34}]$ with *symbols* as indicated in each graph and with mean ± SE ($n = 3$–10). $^*P < 0.05$, $^{**}P < 0.01$, compared with CaM or CaM_{34} binding to NT at the corresponding CaM or CaM_{34} concentration with Ca^{2+}-free condition for (**b**) and (**d**), respectively

Table 2 Fitting parameters for the bindings of CaM and CaM_{34} to NT

	CaM				CaM_{34}			
	EGTA	100 nM	10 μM	2 mM	EGTA	100 nM	10 μM	2 mM
K_d (μM)	0.10	0.02	5.00	0.77	0.12	0.04	1.24	0.98
B_{max} (mol/mol)	0.02	0.02	0.20	0.33	0.02	0.02	0.16	0.27
R^2 (one-site model)	0.910	0.982	0.952	0.983	0.957	0.988	0.922	0.977

Data from the GST pull-down assay shown in Fig. 4 were analyzed with SigmaPlot 10.0 and with a single Hill equation (see "Materials and Methods"). Parameters are similar to those in Table 1

the individual sequences contribute to a single CaM binding site. In the study of Mori et al. [13], L-type channels were fused to a single CaM molecule, and the results suggested that one CaM appears to be both necessary and sufficient to produce CDI for its associated channel. On the other hand, a crystallographic study suggested that more than one molecule of CaM can simultaneously bind to the C-terminal tail peptide of $Ca_V1.2$ [14]. Using a semi-quantitative pull-down method, Asmara et al. [15] also suggested that about two CaM molecules could bind to the

longer C-terminal fragment of $Ca_V1.2$ comprising the preIQ and IQ regions.

Employing a similar pull-down assay method in the present study, we have found that the maximal binding of CaM with the C-terminal tail of $Ca_V1.2$, estimated as $B_{max_1} + B_{max_2}$, is over 1 mol/mol CaMs/peptide for all the four CaMs studied (Table 1). Since the C-terminal tail of $Ca_V1.2$ has more than one CaM binding site, and since CaM has two lobes, each of which can separately bind to the CaM binding sites of the binding partners [5, 18], it is reasonable to speculate that the $Ca_V1.2$ channel may have the capability to bind more than one CaM molecule. In particular, crystal experiments confirmed the existence of a complex constituted by two channels bound with four CaM molecules, although not all the lobes of CaMs are visible [14]. By considering the examined CaM and Ca^{2+} concentration ranges, it was observed that for wild-type CaM the binding ratio higher than 1 happens when $[Ca^{2+}]$ is higher than 10 μM and CaM concentration is higher than 1 μM (Fig. 2). Considering that the physiological concentrations of Ca^{2+} and CaM are less than 2 mM [2] and less than 10 μM [19], respectively, it is likely that, under physiological conditions from resting to earlier exciting, the channel may bind less or one CaM molecule. When Ca^{2+} and CaM concentrations increase further, such as when the cells are fully excited or Ca^{2+} is overloaded under pathophysiological condition, the C-terminal tail of the $Ca_V1.2$ channel may bind more than one CaM molecule. Additionally, provided that $Ca_V1.2$ channel in situ has a higher affinity than that observed with its fragment peptides in vitro, it may be possible that multiple molecules of CaM play a role in Ca^{2+}-dependent regulation of the channel in physiological conditions.

It has been suggested that C- and N-lobes of CaM have distinct roles in the regulation of Ca^{2+} channels [6, 11, 12, 18]. It is reported that the C-lobe, when bound with Ca^{2+}, triggers a rapid CDI process, whereas the N-lobe induces a distinct and relatively slow CDI in $Ca_V1.2$ channels [9]. Recently, a patch-clamp study showed that both N- and C-lobes of CaM are required for the Ca^{2+}-dependent regulation of $Ca_V1.2$ channels [20, 21]. Thus, the role of each lobe of CaM remains to be elucidated. Although we demonstrated that all the three CaM mutants could bind with the CT1 peptide of $Ca_V1.2$ (Figs. 2, 3), the concentration-binding curve for CaM_{12} shifted slightly upward with increasing $[Ca^{2+}]$, which is similar to that of wild-type CaM (Fig. 2). On the other hand, there was no significant shift for those of CaM_{34} and CaM_{1234} (Fig. 3), suggesting that the C-lobe of CaM plays a dominant role in triggering the Ca^{2+}-dependent regulation of $Ca_V1.2$.

Besides the C-terminal tail of the $Ca_V1.2$ channel, CaM has been reported to interact with the N-terminal tail [9, 15]. The functional significance of this region has been demonstrated for $Ca_V1.2$ in vivo by patch-clamp technique [9]. In this study, we have confirmed that CaM and CaM_{34} could bind to NT at $[Ca^{2+}] \geq 10$ μM (Fig. 4). These results may imply that the Ca^{2+}-bound N-lobe of CaM may play an important role in the binding of CaM to NT, and this idea is consistent with the hypothesis that CaM can bridge N- and C-terminal tails of $Ca_V1.2$ channel [9].

Based on the present and other data, we propose a hypothesis for the Ca^{2+}/CaM-dependent regulation of $Ca_V1.2$ channels. At low and middle levels of $[Ca^{2+}]$, $Ca_V1.2$ channel may usually bind one CaM molecule, and its Ca^{2+}-dependent regulation may be predominately conducted by the C-lobe of CaM. A Ca^{2+}-dependent increase in the extent of CaM-bound channel may underlie CDF of the channel [20, 21]. When Ca^{2+} and CaM concentrations increased, the channel may bind with the second CaM molecule at its C terminal tail, and this may be related to CDI of the channel. However, we do not exclude the alternative possibility that the N-terminal tail of $Ca_V1.2$ binds with N-lobe while the C-terminal tail of the channel binds C-lobe of CaM (bridge formation), providing another conformation of CDI [9]. It is to be examined in future studies which conformation for CDI is occurring in the intact cells.

Acknowledgments This work was supported by grants from the Natural Science Foundation of China (31071004, 81001429 and 81100108), and grants-in-aid from the Ministry of Education, Culture, Sports, Science and Technology of Japan (21390059 and 23790251).

Conflict of interest The authors declare that they have no conflict of interest.

References

1. Catterall WA (2000) Structure and regulation of voltage-gated Ca^{2+} channels. Annu Rev Cell Dev Biol 16:521–555
2. Chin D, Means AR (2000) Calmodulin: a prototypical calcium sensor. Trends Cell Biol 10:322–328
3. Zühlke RD, Pitt GS, Tsien RW, Reuter H (1999) Calmodulin supports both inactivation and facilitation of L-type calcium channels. Nature 399:159–162
4. Blaich A, Pahlavan S, Tian Q, Oberhofer M, Poomvanicha M, Lenhardt P, Domes K, Wegener JW, Moosmang S, Ruppenthal S, Scholz A, Lipp P, Hofmann F (2012) Mutation of the calmodulin binding motif IQ of the L-type Ca(v)1.2 Ca^{2+} channel to EQ induces dilated cardiomyopathy and death. J Biol Chem 287:22616–22625
5. Pitt GS, Zühlke RD, Hudmon A, Schulman H, Reuter H, Tsien RW (2001) Molecular basis of calmodulin tethering and Ca^{2+}-dependent inactivation of L-type Ca^{2+} channels. J Biol Chem 276:30794–30802
6. Peterson BZ, DeMaria CD, Adelman JP, Yue DT (1999) Calmodulin is the Ca^{2+} sensor for Ca^{2+}-dependent inactivation of L-type calcium channels. Neuron 22:549–558
7. Zühlke RD, Reuter H (1998) Ca^{2+}-sensitive inactivation of L-type Ca^{2+} channels depends on multiple cytoplasmic amino

acid sequences of the α_{1C} subunit. Proc Natl Acad Sci USA 95:3287–3294
8. Kim J, Ghosh S, Nunziato DA, Pitt GS (2004) Identification of the components controlling inactivation of voltage-gated Ca^{2+} channels. Neuron 41:745–754
9. Dick IE, Tadross MR, Liang H, Tay LH, Yang W, Yue DT (2008) A modular switch for spatial Ca^{2+} selectivity in the calmodulin regulation of Ca_V channels. Nature 451:830–834
10. Benmocha A, Almagor L, Oz S, Hirsch JA, Dascal N (2009) Characterization of the calmodulin-binding site in the N terminus of $Ca_V1.2$. Channels (Austin) 3:337–342
11. DeMaria CD, Soong TW, Alseikhan BA, Alvania RS, Yue DT (2001) Calmodulin bifurcates the local Ca^{2+} signal that modulates P/Q-type Ca^{2+} channels. Nature 411:484–489
12. Liang H, DeMaria CD, Erickson MG, Mori MX, Alseikhan BA, Yue DT (2003) Unified mechanisms of Ca^{2+} regulation across the Ca^{2+} channel family. Neuron 39:951–960
13. Mori MX, Erickson MG, Yue DT (2004) Functional stoichiometry and local enrichment of calmodulin interacting with Ca^{2+} channels. Science 304:432–435
14. Fallon JL, Baker MR, Xiong L, Loy RE, Yang G, Dirksen RT, Hamilton SL, Quiocho FA (2009) Crystal structure of dimeric cardiac L-type calcium channel regulatory domains bridged by Ca^{2+} calmodulins. Proc Natl Acad Sci USA 106:5135–5140
15. Asmara H, Minobe E, Saud ZA, Kameyama M (2010) Interactions of calmodulin with the multiple binding sites of $Ca_V1.2$ Ca^{2+} channels. J Pharmacol Sci 112:397–404
16. Minobe E, Asmara H, Saud ZA, Kameyama M (2011) Calpastatin domain L is a partial agonist of the calmodulin-binding site for channel activation in $Ca_V1.2$ Ca^{2+} channels. J Biol Chem 286:39013–39022
17. Xiong L, Kleerekoper QK, He R, Putkey JA, Hamilton SL (2005) Sites on calmodulin that interact with the C-terminal tail of $Ca_V1.2$ channel. J Biol Chem 280:7070–7079
18. Van Petegem F, Chatelain FC, Minor DL Jr (2005) Insights into voltage-gated calcium channel regulation from the structure of the Ca_V 1.2 IQ domain-Ca^{2+}/calmodulin complex. Nat Struct Mol Biol 12:1108–1115
19. Black DJ, Tran QK, Persechini A (2004) Monitoring the total available calmodulin concentration in intact cells over the physiological range in free Ca^{2+}. Cell Calcium 35:415–425
20. Han DY, Minobe E, Wang WY, Guo F, Xu JJ, Hao LY, Kameyama M (2010) Calmodulin- and Ca^{2+}-Dependent Facilitation and Inactivation of the $Ca_V1.2$ Ca^{2+} Channels in Guinea-Pig Ventricular Myocytes. J Pharmacol Sci 112:310–319
21. Guo F, Minobe E, Yazawa K, Asmara H, Bai XY, Han DY, Hao LY, Kameyama M (2010) Both N- and C-lobes of calmodulin are required for Ca^{2+}-dependent regulations of $Ca_V1.2$ Ca^{2+} channels. Biochem Biophys Res Commun 391:1170–1176